THEORETICAL EFFECT OF VARIOUS BROADENING PARAMETERS ON ULTRAVIOLET LINE PROFILES

Eric Peytremann
Smithsonian Astrophysical Observatory
Cambridge, Massachusetts

ABSTRACT

We study the relative importance of various damping parameters in ultraviolet lines under conditions of normal stellar atmospheres ($10{,}000°K \leq T_{eff} \leq 30{,}000°K$, $\log g = 4$). It is found that the damping by electron collisions is always much smaller than either the radiative or the classical damping, except for lines that arise from high-excitation levels and do not therefore develop strong damping wings. A damping constant equal to 10 times the classical value is always much too large when compared to the more realistic (electron + radiative) damping.

I. INTRODUCTION

The spectra of O and B stars show a large number of metallic lines in the ultraviolet region of the spectrum — that is, between the Lyman limit and approximately 2000 Å. We refer the reader to the results presented at the IAU Symposium 36 (Houziaux and Butler, 1970). Some of these lines are so strong that they can be observed with a resolution as low as 10 Å (Code and Bless, 1970). These strong lines can be heavily saturated and hence develop important damping wings. So one must pay some attention to the damping parameters that one is going to use in line-profile calculations. In addition to the ordinary spectral analysis of each individual line, calculation of the wings of these strong lines must be carried out carefully because (a) they may account for a nonnegligible fraction of the total blanketing effect, and (b) they may block out a substantial amount of energy from the spectral

ranges (narrow or broad) to which they belong. Point (a) concerns the structure of atmospheric models, and (b) relates to the effects of these lines on such observable quantities as low-resolution spectroscopy, or narrow-to-broad-band photometry. Earlier attempts to calculate blanketed models with ultraviolet lines have included a damping constant equal to 10 times its classical value (see Adams and Morton, 1968; Hickok and Morton, 1968; Bradley and Morton, 1969; Wayne van Citters and Morton, 1970). The reason is perhaps that their value represents empirically rather well the damping in solar-type atmospheres. But under solar conditions, the broadening by collisions with neutral particles is a predominant damping mechanism, whereas in the hotter atmospheres studied here, it is not. In this paper, we compare various damping parameters and from them calculate a number of line profiles. The range of temperatures considered is such that damping by collisions with neutral hydrogen can be neglected — that is, the temperatures are representative of model atmospheres with effective temperature T_{eff} larger than 10,000°K. The upper limit of the temperature range has been taken equal to T_{eff} = 30,000°K because in hotter atmospheres, the effects of non-LTE are expected to be very large (Mihalas and Auer, 1970).

II. DAMPING PARAMETERS

For metallic lines, which are the only ones considered in this study, we shall consider two damping mechanisms:

1. Natural, or radiative, damping γ_R, which, for a line with upper level u and lower level ℓ, is given by

$$\gamma_R = \sum_{E_i<E_\ell} A_{\ell i} + \sum_{E_j<E_u} A_{uj} \quad . \qquad (1)$$

Here, the $A_{\ell i}$'s are the transition probabilities from level ℓ to level i, and A_{uj}, from level u to level j, measured in sec^{-1}. The summations are carried over all levels i lower than level ℓ, and all levels j lower than u. The line-opacity profile is Lorentzian, with damping constant γ_R.

2. Broadening by electron collisions. According to Sahal-Bréchot (1969a,b) and to Chapelle and Sahal-Bréchot (1970), the impact approximation is valid for electron collisions under the conditions of normal stellar atmospheres. Hence, the line-opacity profile is Lorentzian, with a damping parameter γ_e (sec^{-1}), where γ_e is proportional to the number density of the perturbers, that is to the electron density N_e (cm^{-3}).

Because both these broadening mechanisms give rise to Lorentzian profiles, the resulting profile is Lorentzian, with damping γ equal to

$$\gamma = \gamma_R + \gamma_e \quad (\text{sec}^{-1}) \ . \tag{2}$$

The damping due to collisions with protons or He^+ ions is much less than the electron damping (Sahal-Bréchot and Segré, 1970). As we shall see, the electron damping itself plays a minor role in all cases where damping wings are strong. Hence, we neglect the damping due to collisions with H^+ and He^+ ions. We shall also compare the radiative and electron damping to the classical damping γ_C,

$$\gamma_C = 0.221 \times 10^{16}/\lambda^2 \quad (\text{sec}^{-1}) \ , \tag{3}$$

where λ is the wavelength of the line in angstroms. A number of model atmospheres with ultraviolet line blanketing have been computed with 10 times γ_C, the value of Morton and his coworkers cited earlier. Because the classical value for damping is easy to compute, it would be useful to derive an empirical value of the damping constant as a multiple of γ_C, for the following reasons. First, the computation of line-blanketing effects involves lengthy calculations (hundreds or thousands of lines); it is desirable to keep the number within reasonable limits. Second, for many of these lines, the data for γ_R and γ_e are simply unavailable. If, however, the radiative damping γ_R and the electron damping γ_e are available for the very strong lines, we can make the following predictions. If γ_R is predominant, the damping mechanism does not give any information on the properties of the atmosphere, because γ_R is essentially an intrinsic atomic parameter. On the other hand, if γ_e is predominant, the damping part of the line profiles would give us information on the state of the gas, mainly the electron density and only slightly, the temperature. This information would then play the role of a gravity indicator.

To carry out these various comparisons, we selected those multiplets for which the necessary data were available. These data, together with some other basic line data, are displayed in Table 1. For each multiplet, we indicate the name of the ion in the first column, followed by the abundance by number log ε (with log $\varepsilon(H) = 12$), the ionization potential χ(in ev), the wavelengths λ(Å), and the oscillator strengths log gf of each multiplet's lines. Next, we give the excitation potentials (in ev) of the lower (χ_ℓ) and upper (χ_u) levels. Finally, the last three columns contain the electron damping $C_e = 10^6\ \gamma_e/N_e$ at T = 20,000°K, the radiative damping γ_R, and

Table 1. $C_e = (\gamma_e/N_e \times 10^6)_{T = 20{,}000°K}$

Ion	log ε	χ(ev)	λ(Å)	log gf	χ_ℓ	χ_u	C_e	γ_R × 10^{-8}	γ_c
C II	8.50	24.38	1334.53	-0.28	0	9.29	0.3	5.9	12.5
			1335.66	-0.97					
			1335.71	-0.02					
C IV	8.50	64.48	1548.20	-0.42	0	8.01	0.5	2.6	9.3
			1550.77	-0.72					
N II	8.00	29.59	1083.98	-0.77	0	11.43	0.3	5.8	18.9
			1084.57	-0.42					
			1084.57	-0.90					
			1085.50	-2.07					
			1085.54	-0.90					
			1087.70	-0.15					
Si II	7.50	16.34	1260.42	0.38	0	9.83	2.7	30.0	14.0
			1264.73	0.63					
			1265.02	-0.32					
			1304.37	-0.44	0	9.50	0.5	10.6	13.0
			1309.27	-0.74					
			1526.72	-0.59	0	8.12	2.0	11.1	9.5
			1533.45	-0.28					
			1808.00	-1.89	0	6.86	0.5	0.1	6.8
			1816.92	-1.63					
			1817.45	-2.60					
			2500.93	-0.67	9.83	14.79	93.6	31.1	3.6
			2501.97	-0.51					
			2502.00	-1.82					
			2904.28	-0.29	9.83	14.10	35.9	32.2	2.6
			2905.69	-0.14					
			2905.70	-1.44					

Table 1, continued

Ion	log ε	χ(ev)	λ(Å)	log gf	χ_ℓ	χ_u	C_e	$\gamma_R \times 10^{-8}$	$\gamma_c \times 10^{-8}$
Si III	7.50	33.46	993.52	-0.93	6.54	19.01	1.3	23.6	22.4
			994.79	-0.45					
			997.39	-0.23					
			1108.37	-0.05	6.54	17.72	0.9	29.1	18.1
			1109.94	-0.18					
			1109.97	0.32					
			1113.17	-1.35					
			1113.20	-0.18					
			1113.23	0.57					
			1206.51	0.23	0	10.27	1.1	23.6	15.3
			1294.54	-0.15	6.55	16.13	1.8	22.3	13.2
			1296.73	-0.25					
			1298.89	-0.37					
			1298.96	0.32					
			1301.15	-0.25					
			1303.32	-0.15					
			1206.53	0.73	10.27	20.55	2.2	74.5	15.2
			2541.82	-0.81	10.27	15.15	1.1	26.2	3.4
Si IV	7.50	45.13	1066.63	0.97	19.88	31.50	4.0	65.5	19.5
			1122.49	0.22	8.84	19.88	1.0	35.6	17.6
			1128.33	-0.48					
			1128.34	0.48					
			1393.76	0.03	0	8.89	1.0	9.2	11.4
			1402.77	-0.27					
			1533.22	0.25	30.99	39.07	44.0	23.9	9.4
			1796.16	-0.82	30.99	37.89	17.0	13.5	6.9
			1790.17	-1.77					
			1797.50	-1.08					

the classical damping γ_C. The two latter are in units 10^{-8} sec^{-1}, and γ_C has been calculated according to equation (3).

The values of the electron damping have been taken from Sahal-Bréchot and Segré (1970). It should be noted that the temperature dependence of γ_e is weak. In most cases of interest, γ_e varies like $T^{-0.25}$. Also, the damping γ_e is the same for all lines of a given multiplet (Chapelle and Sahal-Bréchot, 1970).

The radiative damping γ_R has been calculated according to equation (1) by searching through the tables of atomic-transition probabilities by Wiese, Smith and Miles (1969) and by Wiese, Smith and Glennon (1966). The log gf values have also been taken from these tables. No critical discussion of the contents of these tables has been attempted. It could be that lifetimes of some levels are missing, which would lead to radiative-damping constants that are too small. (This may be the case of multiplet Si II at λ = 1808 Å.) We give only one value of γ_R for each multiplet because the variations of γ_R within a given multiplet are at most $\pm 0.1 \times 10^8$ (sec^{-1}).

Before we discuss these various damping parameters, we describe Figure 1. It shows the damping log γ_e and log γ_R for each multiplet of Table 1 (in units sec^{-1}). The open circles indicate the electron damping, and the crosses the radiative damping. Each multiplet is labeled by its wavelength. The γ_e is for an electron density $N_e = 10^{14}$ (cm^{-3}) and a temperature T = 20,000°K. This density corresponds to rather high values of the optical depth ($\tau_{5000} \simeq 1$) in atmospheres with a gravity log g = 4 and $T_{eff} > 10{,}000$°K. In shallower layers, where the lines are more likely to be formed, the electron damping would be lower. And in atmospheres with lower gravities, it would be still lower. Thus, the values of γ_e in Figure 1 must be considered as upper limits in most cases of astrophysical interest. Also shown in Figure 1 is the classical damping γ_C, together with 10 times γ_C, as a function of wavelength.

From Table 1 and Figure 1, we can easily draw the following conclusions:

1. The electron damping is nearly always lower than the radiative damping, even with the rather high value of $N_e = 10^{14}$(cm^{-3}). The only lines for which the electron damping is important are those arising between very highly excited levels. Hence, these lines are not strong, and damping does not play an important role.

2. For most lines whose lower level is not too highly excited (and which may therefore be very strong), the radiative damping is between 1/3 and 3 times the classical damping. One exception is the already mentioned multiplet of Si II at

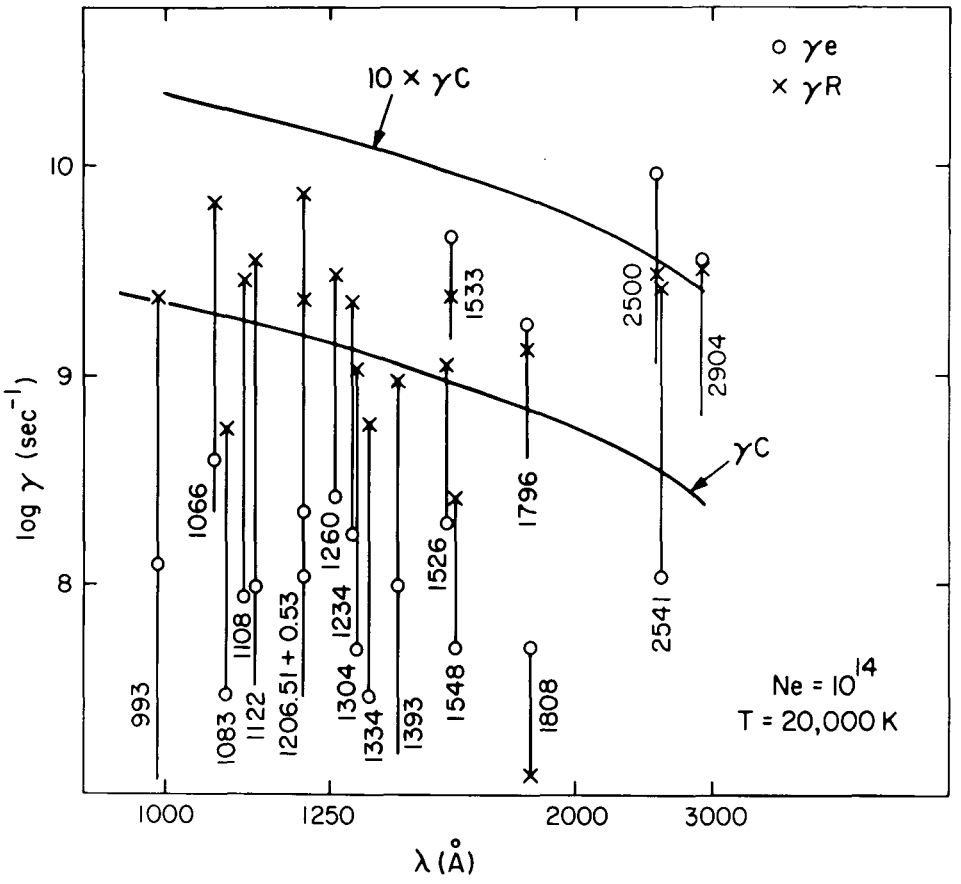

Figure 1.—Damping log γ of a number of ultraviolet multiplets. Crosses indicate radiative damping. Open circles indicate electron damping. The data of each multiplet are labeled with its wavelength. Solid lines show classical and 10 times classical damping.

λ = 1808 Å.

3. For all lines that qualify to develop strong damping wings, the value $\gamma = 10\ \gamma_C$ is much too large, by a factor 3 at least, with respect to either γ_R or $\gamma = \gamma_R + \gamma_e$.

4. The radiative damping being predominant, we do not expect any gravity effect on the line profiles via the damping mechanism. This answers the question that we raised previously.

III. ULTRAVIOLET LINE PROFILES AND EQUIVALENT WIDTHS

In this section, we consider how our various damping parameters influence the profiles and equivalent widths of strong lines. These lines are supposed to be formed in stellar

atmospheres with effective temperatures T_{eff} ranging from 10,000 to 30,000°K and with a surface gravity log g = 4. However, because we want to study the relative effects of the damping parameters with respect to each other, we do not worry too much about the degree of realism of our computations (i.e., abundances, microturbulence, etc.). So we simply indicate how the calculations have been performed, without any critical discussion of matters not directly related to the damping problem.

To calculate our line profiles, we used the program ATLAS (Kurucz, 1969), modified to calculate metallic-line profiles and equivalent widths (Peytremann, 1970). The basic assumptions are those of classical model atmospheres: plane-parallel and in hydrostatic and radiative equilibrium. Occupation numbers are given by the Saha-Boltzmann relations. The source function is calculated according to the Milne-Eddington relation, with scattering by free electrons. (Rayleigh scattering is negligible at these high temperatures.) The line opacities are treated in pure absorption. With these assumptions, it is clear that the line cores are incorrect, but they are rather narrow as compared to the strong damping wings. As stated previously, we are currently interested in these damping wings, and it is precisely these that contribute mostly to the equivalent widths of strong lines, as we shall see later.

The line-opacity profiles are given by Voigt functions calculated according to Baschek, Holweger, and Traving (1966). At each frequency, we sum up the continuous opacities and the opacities of all the relevant lines (blends). In our case, we take into account all lines of a given multiplet. Also, for clarity, we do not include the opacities of nearby hydrogen lines. The equivalent widths have been computed according to Baschek et al. (1966) with the following exception. Most of the lines studied here are so broad that the residual fluxes

$$r_\lambda = F(\lambda)/F_c(\lambda) \qquad (4)$$

are calculated with respect to the continuum $F_c(\lambda)$ and not, as usual, to the continuum at the line-center wavelength ($F(\lambda)$ is the flux in the line, and $F_c(\lambda)$ is the continuum flux). However, since the computation of the flux at each frequency point is time consuming, we calculate only three continuum points for each multiplet and obtain the $F_c(\lambda)$ values by parabolic interpolation. This completes our description of the computational method.

The actual data entering the computations are (a) the model atmospheres and (b) the line data. (a) The models are hydrogen line-blanketed models calculated with the unmodified pro-

gram ATLAS (Kurucz, 1969). The ratio of helium to hydrogen by number is equal to 1/9. At our temperature ($10{,}000 \geq T_{eff} \geq 30{,}000°K$), metals are unimportant as electron donors. The gravity has been taken as log g = 4. As we shall see, the effect of the electron density (and hence of the gravity) is so weak that no attempt has been made to calculate line profiles at lower gravities, where the contribution of the electron broadening would be still weaker. Finally, the ad hoc microturbulence parameter that enters the Voigt function has been set equal to 5 km sec^{-1}. The strong lines studied here depend very little on the microturbulence velocity, because their damping wings are far broader than the Doppler core, and some calculations with velocities equal to 0 and 10 km sec^{-1} have indeed confirmed this. (b) The line data are contained in Table 1. The actual values of the abundances and of the partition functions are those contained in our version of the program ATLAS (Peytremann, 1970).

IV. RESULTS AND DISCUSSION

We did not calculate the profiles of all the lines listed in Table 1, at each temperature. In Figures 2 to 9, we display typical results. At the present time, we cannot compare our results to observations, because, for one reason, the instrumental profiles must be known in order to fold them into the theoretical profiles. Moreover, the definition of observed residual fluxes or equivalent widths depends on an accurate definition of the continuum. This is difficult, and perhaps impossible, if the observed spectral feature is blended with a large number of adjacent lines; this indeed is what is observed on ultraviolet spectral scans (Houziaux and Butler, 1970).

Figures 2 and 3 show the profiles of the multiplets λ1083 (N II), and λ1206.51 (Si III). The ordinates are the residual fluxes r_λ defined by (4), and the abscissas give the wavelength in angstroms. The profiles shown here are for models with $T_{eff} = 20{,}000°K$. The various profiles are labeled with γ_e for electron damping, $\gamma_R + \gamma_e$ for electron plus radiative damping, and γ_C for classical damping (Figure 3 only). Also shown are the profiles with 10 times the classical damping. Figure 3 also shows the pure Doppler profile ($\gamma = 0$). It is seen that 10 γ_C gives lines much too broad, as compared to the more realistic $\gamma = \gamma_R + \gamma_e$ case; γ_e alone gives too weak profiles, but its effect is important if we compare it to the zero-damping case ($\gamma = 0$, Figure 3). Figure 2, which displays a six-component multiplet, shows a striking difference between the cases γ_e and $(\gamma_e + \gamma_R)$ and the case 10 γ_C. Whereas the former profiles are resolved into four components, the

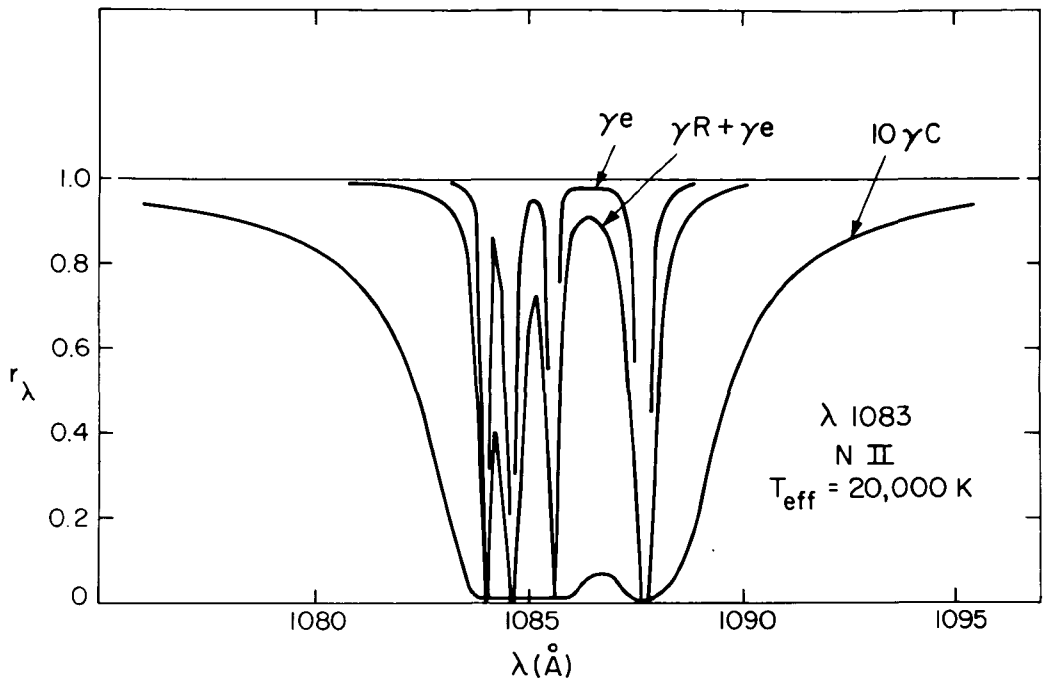

Figure 2.—Profiles of the multiplet of N II at λ = 1083 Å, for a model with T_{eff} = 20,000°K. γ_e, $\gamma_R + \gamma_e$, and 10 γ_C label profiles calculated with electron, electron plus radiative, and 10 times classical damping, respectively.

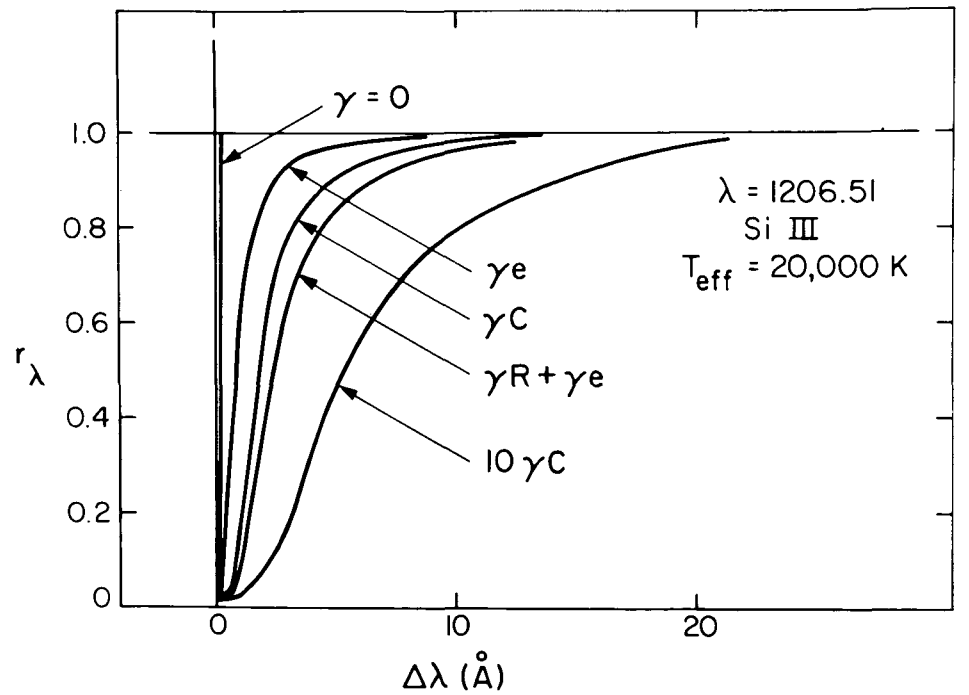

Figure 3.—Same as Figure 2, for a Si III line at 1206.51 Å.

latter does not show any significant resolution of the multiplet's components. To check this, one would need instrumental resolutions on the order of 0.5 Å at $\lambda \simeq 1100$ Å, provided that the multiplet is not blended with other lines.

Figures 4 to 9 show the equivalent widths log W as a function of the effective temperature log T_{eff} of the models. The equivalent widths are in angstroms and are defined as usual by

$$W = \int_0^\infty (1 - r_\lambda) d\lambda \quad , \tag{5}$$

where r_λ has been defined by (4). The various curves are labeled with the same damping parameters given in Figures 2 and 3 and defined in Section 2. Each figure shows the results for a multiplet defined by its wavelength. Also shown are the ion and the number of components of each multiplet (for details, see Table 1). The multiplets of our sample all develop strong damping wings (compare with the pure Doppler case, $\gamma = 0$). Some of them (λ1083, Figure 4; λ1108, Figure 5; λ1206, Figure 6; λ1334, Figure 8) show these strong damping wings over large effective temperature ranges. We reach the same conclusions as in §II and from the analysis of Figures 2 and 3. We note that although the electron damping has little effect, its relative contribution to the total damping $\gamma_R + \gamma_e$ is larger at $T_{eff} = 10{,}000°K$ than at higher temperatures (see, for example, Figures 5 and 6) because in the layers at which the wings of these lines are formed, the electron densities are higher at $T_{eff} = 10{,}000°K$, than at higher temperatures. An indirect consequence is that if any non-LTE effects exist in these regions of line-wing formation, they would be enhanced at higher temperatures.

We now summarize. As stated before, the conditions considered here are those that prevail in atmospheres hotter than, say, 10,000°K, that is, where collision broadening by neutral particles is negligible.

First a damping constant of 10 times the classical value is much too large, by comparison with the more realistic case of electron-plus-radiative damping. This is not necessarily true for lines whose lower level is highly excited, but these lines are not expected to form strong damping wings anyway.

Second, for the strong lines we are dealing with, the effect of electron damping is generally much smaller than that of radiative damping. So we do not expect observable gravity effects due to the broadening mechanisms.

Third, in most cases studied here, the electron-plus-radiative damping gives more or less the same results as the classical damping. Compared to many other sources of errors, these differences are not dramatic. For calculations that

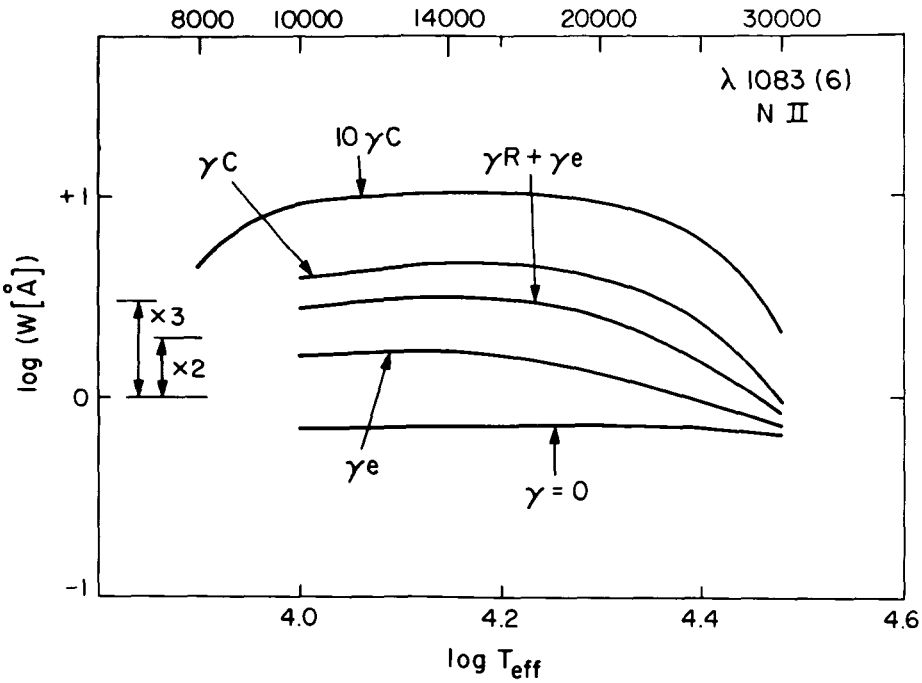

Figure 4.—Equivalent widths log W as a function of effective temperature T_{eff}. W is in angstroms. Multiplet of N II at 1083 Å. The curves are labeled with the damping parameters defined in the text.

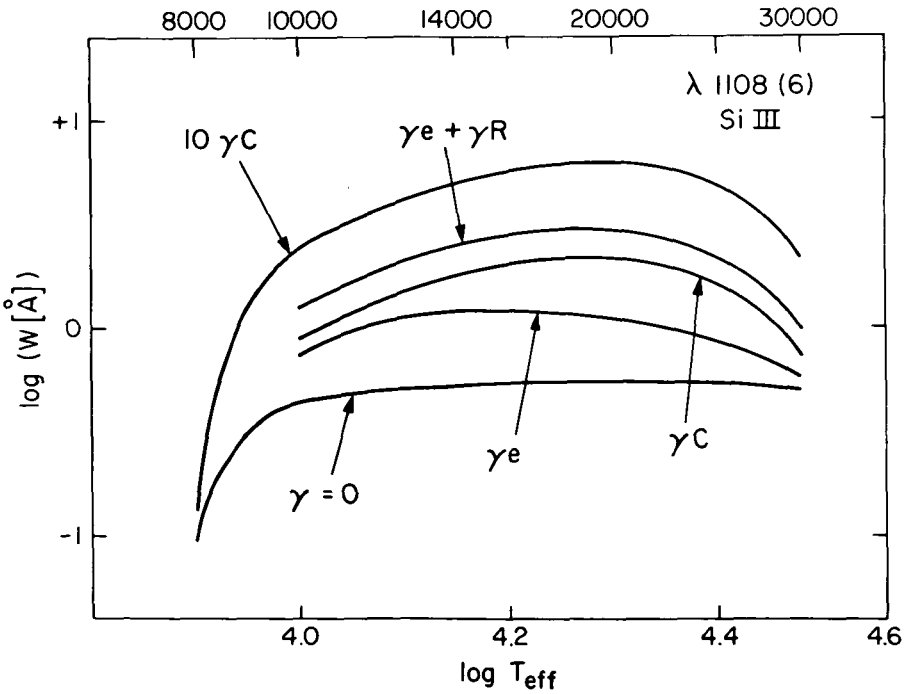

Figure 5.—Same as Figure 4. Multiplet of Si III at 1108 Å.

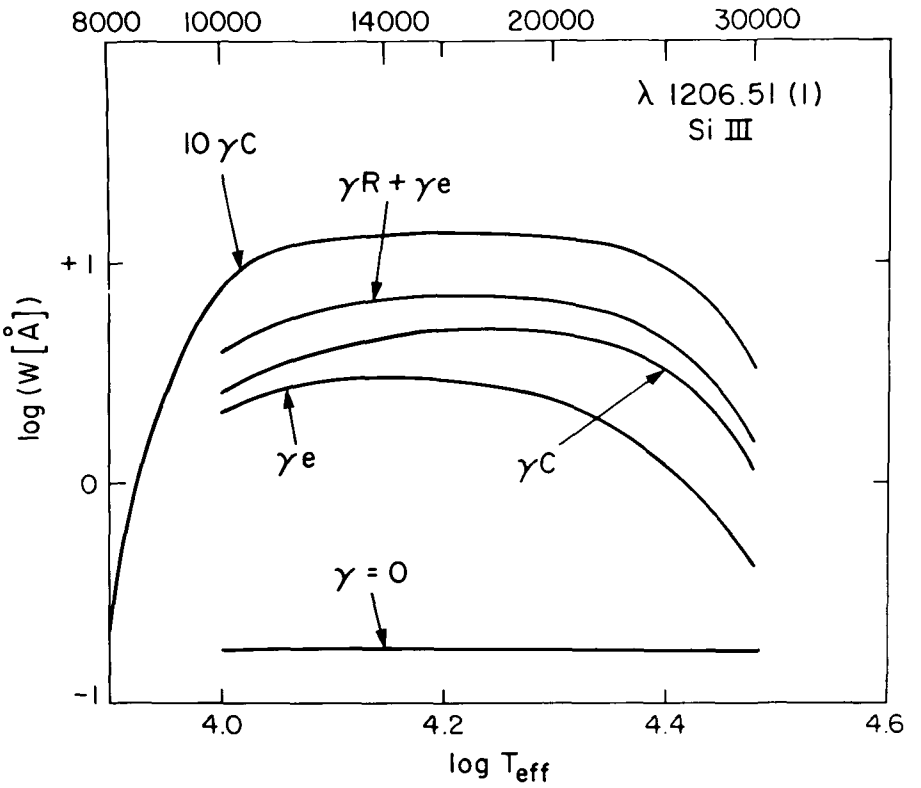

Figure 6.—Same as Figure 4. Multiplet of Si III at 1206.51 Å.

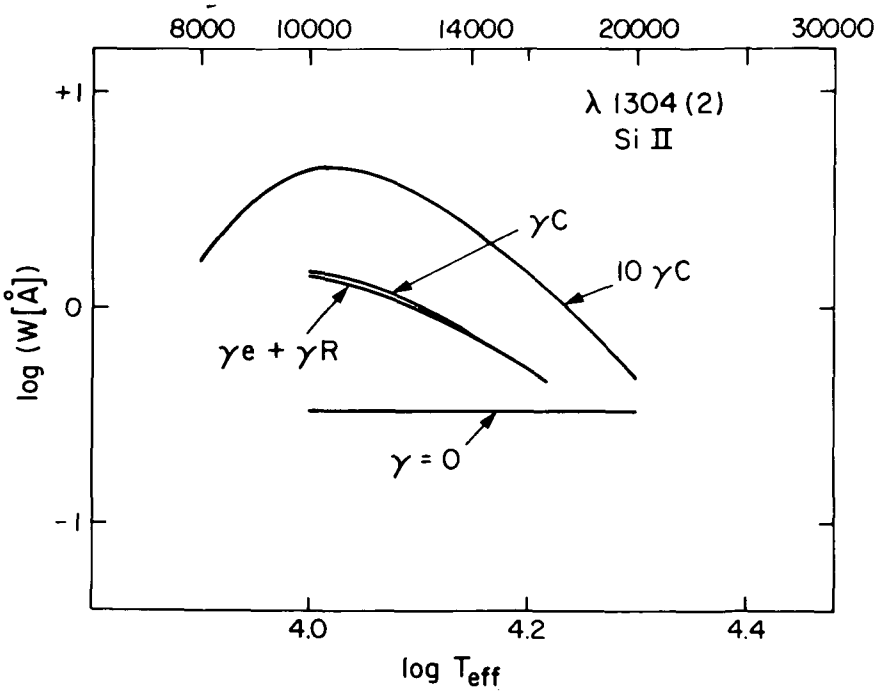

Figure 7.—Same as Figure 4. Multiplet of Si II at 1304 Å.

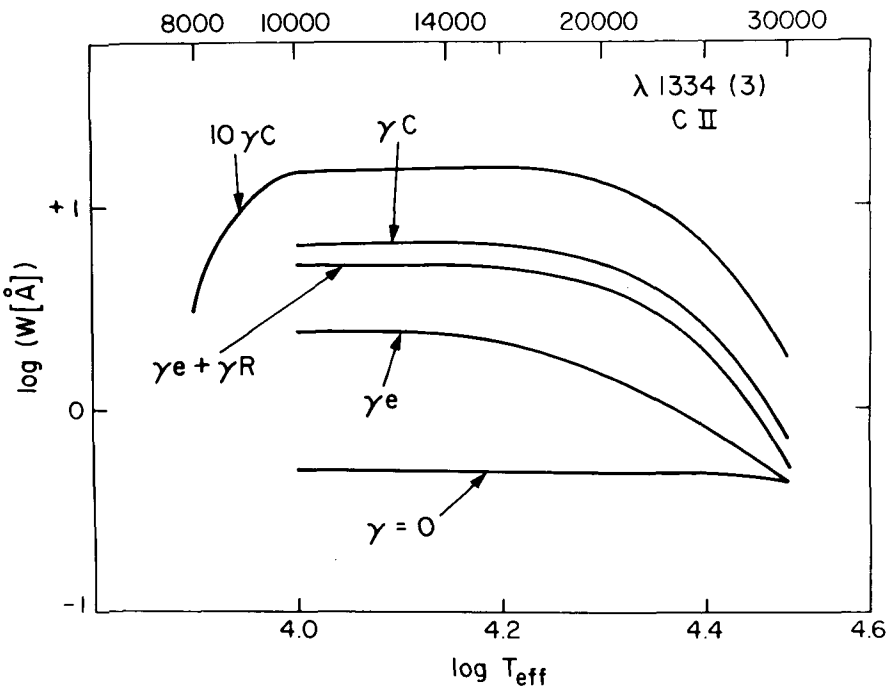

Figure 8.—Same as Figure 4. Multiplet of C II at 1334 Å.

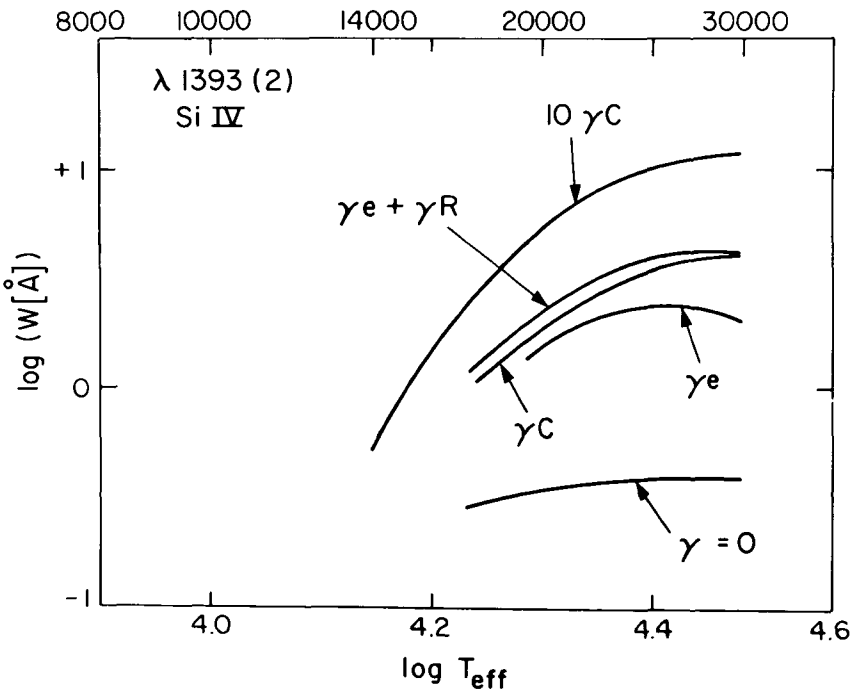

Figure 9.—Same as Figure 4. Multiplet of Si IV at 1393 Å.

involve hundreds or thousands of lines (blanketed model atmospheres) or that concern lines with unavailable damping data, we would therefore suggest, as a rule of thumb, to use the classical damping constant rather than that 10 times greater.

This work has been done while the author held an ESRO-NASA International Fellowship. The research was supported in part by contract NAS 5-1535 from the National Aeronautics and Space Administration.

REFERENCES

Adams, T. F. and Morton, D. C. 1968, Ap. J. 152, 195.
Baschek, B., Holweger, H. and Traving, G. 1966, Abhandl. Hamb. Sternw. VIII. no. 1.
Bradley, P. T. and Morton, D. C. 1969, Ap. J. 156, 687.
Code, A. D. and Bless, R. C. 1970, in Ultraviolet Stellar Spectra and Related Ground-Based Observations (Dordrecht: D. Reidel Publ. Co.) p. 173.
Chapelle, J. and Sahal-Bréchot, S. 1970, Astr. and Ap. 6, 415.
Hickok, F. R. and Morton, D. C. 1968, Ap. J. 152, 203.
Houziaux, L. and Butler, H. E., eds. 1970, in Ultraviolet Stellar Spectra and Related Ground-Based Observations (Dordrecht: D. Reidel Publ. Co.).
Kurucz, R. L. 1969, in Theory and Observation of Normal Stellar Atmospheres, ed. O. Gingerich (Cambridge: M. I. T. Press), p. 375.
Mihalas, D. and Auer, L. H. 1970, Ap. J. 160, 1161.
Peytremann, E. 1970, Thesis, Université de Genève.
Sahal-Bréchot, S. 1969a, Astr. and Ap. 1, 91.
_____ 1969b, Astr. and Ap. 2, 322.
Sahal-Bréchot, S. and Segré, E. 1970, to be published in Highlights for Astronomy.
Wayne van Citters, G. and Morton, D. C. 1970, Ap. J. 161, 695.
Wiese, W. L., Smith, M. W. and Glennon, B. M. 1966, NSRDS-NBS, 4.
Wiese, W. L., Smith, M. W. and Miles, B. M. 1969, NSRDS-NBS, 22.